

## ABSTRACT

### Marine Fish Productivity Across the Paleocene-Eocene Thermal Maximum

Daniel E. Gaskell

Director: Rena Bonem, Ph.D.

The Paleocene-Eocene Thermal Maximum (PETM), a transient global warming event ~55 Ma, is one of the closest geologic analogues to modern-day climate change. Although the PETM is known to have triggered extinctions in deep-sea ecosystems and extensive biogeographic shifts, little work has been done on the response of higher-order marine vertebrates. This work presents mass accumulation data for fossil fish teeth (ichthyoliths) in three ODP/IODP pelagic sediment cores. In all three records, the initial stages of the PETM are associated with a significant transient increase in fish productivity, which may have peaked approximately 10,000 to 15,000 years after the onset of the PETM; the highest resolution data, from the Atlantic, suggests that this increase may have come after a period of significantly depressed productivity. Changes in net primary productivity, as determined from biogenic barium proxies, do not appear sufficient to fully explain the observed trends.

APPROVED BY DIRECTOR OF HONORS THESIS:

---

Dr. Rena Bonem, Department of Geology

APPROVED BY THE HONORS PROGRAM:

---

Dr. Andrew Wisely, Director

DATE: \_\_\_\_\_

MARINE FISH PRODUCTIVITY ACROSS THE PALEOCENE-EOCENE  
THERMAL MAXIMUM

A Thesis Submitted to the Faculty of  
Baylor University  
In Partial Fulfillment of the Requirements for the  
Honors Program

By  
Daniel E. Gaskell

Waco, Texas

May 2015

## TABLE OF CONTENTS

List of Figures . . . . .	3
Acknowledgments . . . . .	4
Chapter One: Introduction . . . . .	1
Chapter Two: Methodology . . . . .	13
Chapter Three: Results . . . . .	23
Chapter Four: Interpretation and Discussion . . . . .	31
Chapter Five: Conclusion . . . . .	44
Bibliography . . . . .	46

## LIST OF FIGURES

Figure 1: Three correction types for 1260B . . . . .	21
Figure 2: Effects of three correction types for 1260B . . . . .	22
Figure 3: 1260B net IAR (Westerhold timescale) – detail . . . . .	26
Figure 4: 1260B net IAR (Murphy timescale) – detail . . . . .	27
Figure 5: 1260B net IAR – full . . . . .	28
Figure 6: 1209C net IAR . . . . .	29
Figure 7: 1220B net IAR . . . . .	30
Figure 8: Core sections for ODP 1209C, 1220B, and 1260B. . . . .	36
Figure 9: Detail of ODP 1220B-20X-02, showing laminations . . . . .	37
Figure 10: Ichthyoliths versus barium: 1209C, 1220B, and 1260B/1051B . . . . .	42
Figure 11: Ichthyoliths versus barium: 1209C, 1220B, and 1260B/1051B . . . . .	43

## ACKNOWLEDGMENTS

I would like to thank Dr. Rena Bonem, for overseeing the development of this thesis, and Professor Richard Norris of the Scripps Institution of Oceanography, for his extensive input and assistance in preparing the ODP 1260B dataset, without which this thesis would not have been possible. I would also like to thank Douglas Tomczik, for providing additional data, and Dr. Steven Driese and Dr. Vince Cronin, for their assistance as second readers.

## CHAPTER ONE

### Introduction

In the coming decades, human-induced climate change has the potential to adversely impact fisheries and marine ecosystems in a multitude of ways (IPCC, 2014, ch. 6). Even without considering long-term consequences to biodiversity, nearly half of the world's population obtain 20% of their annual protein intake from fish (FAO, 2012), and many of the countries most vulnerable to fishery collapse are also among the poorest in the world (Allison and others, 2009). There is an urgent need to understand the impact that global warming will have on fish populations and the overall sustainability of the oceans.

One way to learn about the future is to look to the past. Climate change is not a new phenomenon: by examining geologic data from past intervals of global warming, we can observe the ecological effects of global warming directly. This work uses fossil evidence from one such interval, the Paleocene-Eocene Thermal Maximum (PETM), to compile the first high-resolution record of how global fish populations respond to global warming.

The remainder of this chapter is divided roughly into two parts: first, a general introduction to the PETM and its global consequences; and second, a general introduction to the issues and prior research related to resolving fish populations.

### *The Paleocene-Eocene Thermal Maximum*

The boundary between the Paleocene and Eocene is marked by a rapid and substantial negative carbon isotope excursion (CIE) – averaging -2.8‰ for marine records and -4.7‰ for terrestrial records – as thousands of gigatonnes of isotopically light carbon were released into the atmosphere, prompting rapid and sustained global warming (McInerney and Wing, 2011). This event, which began about 55.8 million years ago (Westerhold and others, 2009; Charles and others, 2011) and lasted about 170,000 years (Röhl and others, 2007), is known as the Paleocene-Eocene Thermal Maximum (PETM).

The PETM is significant as a potential analogue to modern-day global climate change, because the magnitude of carbon release was comparable to that of modern fossil-fuel reserves (Haywood and others, 2011). Research on the PETM has confirmed several fundamental assumptions about climate: large-scale carbon emissions did result in warming and ocean acidification that lasted for tens to hundreds of thousands of years and spurred rapid ecological change (McInerney and Wing, 2011). However, the rate of change was likely an order of magnitude slower than that projected for modern anthropogenic climate change. Thus, the observed ecological disruption should be considered a low-end estimate of potential future impacts (Haywood and others, 2011).

### *Climatic Consequences*

The most obvious consequence of the PETM, as suggested by the name, was thermal: global mean surface temperatures increased by 5-8 °C. The PETM also triggered changes in the hydrological cycle. The increase in continental weathering discussed below is generally attributed to increased precipitation, but chemical and biological proxy data suggest that these changes were the result of increased seasonality



and more intense storms rather than a wetter climate overall. Some regions show sedimentary and faunal evidence of increasingly dry conditions, while others show deposits typical of violent intermittent rainfall (McInerney and Wing, 2011). This hypothesis is consistent with the known pattern of sediment production, which is greatest not under high rainfall, but highly *seasonal* rainfall (Cecil and Dulong, 2003).

Foraminiferal evidence suggests that the PETM coincided with an abrupt shift in deep-water circulation patterns as the dominant region of overturning shifted from the Southern Hemisphere to the Northern Hemisphere, with deep water flowing southwards from the northern Atlantic, rather than northwards from the Southern Ocean. Circulation returned to normal after the CIE (Nunes and Norris, 2006).

### *Biogeochemical Consequences*

*Terrigenous sediment flux.* There is strong evidence that continental silicate weathering increased during the recovery period of the PETM as higher temperatures enhanced the hydrological cycle. Spikes in kaolinite abundance have been noted at a variety of geographically diverse PETM sections, consistent with a warmer and wetter climate producing more thermodynamically stable clays (Kelly and others, 2005), although there is evidence suggesting that this represents increased erosion rather than formation of new clays (McInerney and Wing, 2011). Changes in osmium isotope ratios in seawater require a significant increase in total osmium flux from the continents, suggesting a 20-30% increase in global weathering flux (Ravizza and others, 2001). Sedimentary data from Italy show a bulk sedimentation rate increase of nearly five times in the Forada section and five to ten times in the Tremp Basin, while siliciclastic input

increased by two to five times in the Basque Basin (Giusberti and others, 2007). This increase in weathering and the consequent increase in carbonate precipitation (see below) likely played a role in sequestering atmospheric carbon, facilitating the recovery (Kelly and others, 2005), although the degree and influence of each factor is disputed – contrast, e.g., Ma and others (2014) with Torfstein and others (2010).

These results are consistent with theory. Higher temperatures ease the process of silicate weathering in a predictable manner; more significantly, increased runoff from changes to the hydrological cycle has a strong positive effect on weathering (Kump, and others, 2000). Both conditions were present during the recovery phase of the PETM (Ravizza and others, 2001).

*Ocean productivity.* There is an increasing consensus that primary productivity rose in the recovery stages of the PETM, presumably as a result of increased nutrients from the terrigenous runoff mentioned above (Ma and others, 2014). However, the productivity response of the early stages of the PETM is more complicated and controversial.

One major proxy is barite, which forms as sinking organic matter decomposes at mid water depths (500-2,000 meters); cores from a variety of oceanic regions show two distinctive peaks in barite concentrations, one between 25 and 50 kyr after the start of the event, and one during the recovery phase 75-150 kyr after the start of the event. The precise timing of these peaks is not always constant from site to site. Calculations based on calibrations from modern-day barite formation show that export productivity increased with a range of twofold in the Pacific oligotrophic ocean to fivefold in Equatorial upwelling zones, with an average of threefold (Ma and others, 2014). During the

recovery period, micropaleontological and sedimentological evidence indicates prolific coccolithophore blooms (Kelly and others, 2005).

Trends in the early PETM become less clear when other proxies are considered. Proxies generally agree that open-ocean productivity increased during the recovery phase (Gibbs and others, 2006), but the initial peak is more mixed. Ma and others (2014) point out that at some sites, such as ODP 690, the data appear directly contradictory: barite data show a significant increase in productivity (Bains and others, 2000), whereas nannofossil data show a *decrease* in productivity (Bralower, 2002), and Sr/Ca ratios from coccoliths suggest a minor increase (Stoll and others, 2007). It is probable that different components of ocean productivity became decoupled, so the differing proxies reflect the differing response of each element of the export production process. Further, the validity of each proxy is not always clear: for example, Dickens and others (2003) propose that the barite peak reflects the massive release of barium from methane hydrate reservoirs, rather than a genuine increase in productivity, and Ma and others (2014) propose an increase in mid level decomposition that could artificially increase barite formation. In general, biotic proxies seem to indicate that the onset and peak of the PETM coincided with an increase in productivity along the shelf, and a decrease in productivity in the deep ocean (Gibbs and others, 2006).

*Ocean acidification.* Large releases of CO<sub>2</sub> are expected to be accompanied by large-scale acidification of the ocean (Hönisch and others, 2012). In numerous deep-sea sediment cores, the beginning of the Eocene – and thus the PETM – is marked by a prominent dissolution layer of clay as the carbonate compensation depth (CCD) shoaled by more than two kilometers over a period of less than 10,000 years, recovering gradually

over the next 100,000 years or more. This rapid deep-ocean acidification was a potential contributing factor to the extinction of benthic foraminifera described below (Zachos and others, 2005), although the variety of factors involved precludes the identification of a single cause (Hönsch and others, 2012).

It is unclear to what degree surface waters acidified. The PETM coincides with one of the four major metazoan reef crises of the past 300 million years; but the decline in corallgal reefs was already well underway by the beginning of the Eocene (Hönsch and others, 2012), the existing reefs do not show signs of sudden dissolution (Norris and others, 2013), and calcareous coralline algae actually expanded, contradicting the hypothesis that the coral decline was from lack of binders (Zamagni, Mutti, and Košir, 2012). Coccolithophores and dinoflagellates also show assemblage changes, but it is unclear whether this was the result of acidification or other changes to temperature, salinity, and/or nutrient availability. There does not appear to be a bias against calcified planktic species (Hönsch and others, 2012), as would be expected in the event of significant surface acidification. This has lead to the conclusion that surface-ocean acidification was modest at best (Norris and others, 2013); however, some recent research on boron isotopes in planktic foraminifera has found evidence of a surface pH drop of 0.3 (Penman and others, 2014). Research in this area is ongoing and the true extent of surface-water acidification remains to be seen.

### *Ecological Consequences*

The marine ecological consequences of the PETM have been studied extensively using data from nearly every major marine environment. Work to date has focused almost exclusively on single-celled microfossils such as foraminifera, radiolarians,

diatoms, and calcareous nannofossils (McInerney and Wing, 2011); very little is known about how vertebrates and macroinvertebrates responded to the PETM, hence the contribution of this thesis. Terrestrial ecological consequences cannot normally be studied with the temporal resolution of marine ecology, but the faunal trends of the Eocene, in general, are fairly well understood.

*Benthic ecosystems.* It has long been known that the end of the Paleocene was marked by a large-scale extinction of benthic foraminifera, with 30-50% of species lost. Post-extinction, benthic foraminifera communities were low-diversity and dominated by thin-walled calcareous or agglutinated species (Thomas, 2007). Extinction was greatest at middle bathyal and greater depths (McInerney and Wing, 2011). Three main mechanisms have been proposed: anoxia, increased corrosion, and productivity changes. Each has problems. In the case of anoxia or corrosion, refugia should have remained that would preserve diversity, and the extinctions include species that should have been resistant. In the case of productivity, the response is inconsistent and regional (see above), and it seems improbable that productivity could have such an effect given that no such extinction occurred from similar environments at the end of the Cretaceous. The warming itself seems the most viable trigger, as its global nature would have precluded obvious refugia, but the mechanism by which this might have occurred is unknown (Thomas, 2007).

In addition to the extinction, Alegret and others (2010) find a sharp decrease in maximum benthic test diameter from 0.3 mm to 0.15 mm shortly after the onset of the PETM, which recovers some time after to approximately pre-PETM levels. They suggest this may have resulted from a combination of factors, including higher temperatures

increasing the metabolic rate of benthic foraminifera and leaving insufficient food; by contrast, Kaiho and others (2006) suggest that the primary driver was a rapid drop in dissolved oxygen in bottom water.

*Pelagic ecosystems.* The response of planktic foraminifera varies by species, suggesting a highly complex ocean structure (Alegret and others, 2010). Unlike their benthic counterparts, there was no obvious extinction event. Instead, the PETM is marked by abrupt changes in assemblage composition, such as an increase in the abundance of acarininids relative to morozovellids. Planktic foraminifera also underwent rapid morphological diversification (Kelly and others, 1998), producing a set of distinctive “excursion taxa” that evolved in less than 10,000 years and persisted only until the end of the PETM (McInerney and Wing, 2011).

In contrast to benthic foraminifera, the maximum test diameter of planktic foraminifera increased from 0.60 mm to 0.75 mm before returning to background levels. This may have resulted from an initial drop in surface productivity (see above) that gave an adaptive advantage to larger forams that could carry more algal photosymbionts (Kaiho and others, 2006).

*Terrestrial ecosystems.* The PETM coincides with the first appearances of most modern orders of mammals (Gingerich, 2006), as well as temporary shifts in megaf flora that are generally consistent with seasonal precipitation and greater evaporation from higher temperatures (McInerney and Wing, 2011).

### *Reconstructing Fish Populations*

Very little is known about how fish and other marine vertebrates responded to the PETM. Given the PETM's effect on other secondary and tertiary consumers (such as mammals) and the significant changes to ocean productivity that occurred throughout the interval, it is probable that fish would show a response; yet no direct reconstruction of fish populations across the PETM is currently available. This section provides general background on the methods by which such a record could be compiled, and summarizes the existing data on fish populations during the PETM.

#### *General Observations*

Fossil evidence of fish populations comes mainly from “ichthyoliths,” microscopic fish skeletal debris such as teeth. A variety of sources have incidentally mentioned ichthyolith trends across the Paleocene-Eocene boundary, the most notable of which are several stratigraphic surveys from Egypt. Ouda and Berggren (2003) correlate several boundary records in the Upper Nile Valley and note an abundance of fish remains shortly before the PETM, which apparently disappear at the boundary and reappear shortly after. Another paper (Berggren and Ouda, 2003) describes the Dababiya PETM section in detail and describes approximately the same trend. Yet another paper by Ouda and others (2003) describes a section in the Idfu-Esna area and mention an increase in fish teeth and other phosphatic grains following the onset of the PETM.

Several years later, Tantawy (2006) describes a PETM section in the Central Nile Valley and notes that the dissolution layer at the base of the Eocene is almost entirely devoid of microfossils, but is followed by a dark brown shale full of fish teeth and bones. Soliman (2003) reports a similar trend in another PETM section at Gabal el-Qreiya in the

Nile Valley: after the initial basal clay layer, phosphate grains spike to a high of nearly 20% before returning to less than 1% over the course of the next few samples. More generally, Bornemann and others (2009) primarily examine the Late Danian carbon isotope excursion, but include a table comparing the Late Danian Event (LDE) with the PETM, which notes that both feature abundant fish remains.

The references above are tantalizing but limited. It seems that the following general trend holds for P/E boundary sediments in the Nile Valley:

1. Fish remains are abundant at the end of the Paleocene;
2. The beginning of the Eocene is marked by a clay layer with limited fauna of any kind, including fish remains;
3. Fish remains increase in abundance again in the interval following the clay layer (in some cases quite significantly); and
4. Later Eocene sediments may have comparatively fewer fish remains (see, e.g., Berggren and Ouda, 2003, and Soliman, 2003.)

From these data alone, however, it is not clear whether this sequence represents a genuine population shift or an artifact of the region's depositional history. For example, Ouda and Berggren (2003) propose that the concentration of phosphates in the post-PETM interval may be an artifact of deposition rate and point to changes in the coarse residual fraction (CRF) as evidence of a possible reduction in terrigenous input. By contrast, Soliman (2003) proposes that the phosphate unit represents a series of mortality events, perhaps from periodic upwelling or overturning of anoxic bottom waters. Both of these hypotheses will be discussed further in chapter four.



### *Chemical Proxy Data*

Ichthyoliths are composed mainly of calcium phosphate, so phosphorus content can provide a rough proxy for ichthyolith content. This has the advantage of being much easier to acquire than conventional extraction techniques (as phosphorus content can be measured with automated techniques such as mass spectrometry and X-ray fluorescence.) However, phosphorus is of limited application as a proxy because it has multiple sources; not all the phosphorus in a sample is necessarily from ichthyoliths. Chemical methods have been developed to distinguish between phosphorus associated with biogenic apatite and phosphorus associated with non-biological sources (see, e.g., Schenau and Lange, 2000), but such techniques do not appear to have ever been used on PETM sections. Nevertheless, simple phosphorus measurements can still be useful as a way to compare or support results gathered by more sensitive methods.

One such dataset can be found in Khozyem and others (2013), who report chemical data for the Wadi Nukhul PETM section in Sinai, Egypt. At the beginning of the PETM, phosphorus content decreases from a mean of 2,790 parts per million (ppm) to a low of about 1,000 ppm; at the end of the clay interval, phosphorus content abruptly spikes to 5,498 ppm, before decreasing over the next few centimeters to a new mean of about 1,500 ppm. These data appear consistent with the ichthyolith data discussed above.

### *Opportunities for Further Work*

The datasets discussed above are intriguing but inconclusive. It seems likely that marine vertebrates *did* respond to the PETM, but the magnitude and timing of this response is unclear. This work attempts to address this lack of information by presenting

the first quantitative, high-resolution ichthyolith mass accumulation data across the PETM, obtained from pelagic sediments.

## CHAPTER TWO

### Methodology

This work investigates how fish populations responded to the Paleocene-Eocene Thermal Maximum, using data from ichthyoliths preserved in pelagic ooze. Chapter 2 includes a review of the research design and data collection/processing methods.

#### *Research Questions*

The core question behind this work is: “What does global climate change do to fish?” Using the case study of the PETM, the primary factual questions include:

- What happened to fish populations when global climate changed during the PETM? Were they unaffected, or did they thrive, die, or a combination of both?
- Were there regional differences in population response?
- Does the response correlate directly with primary productivity or any other other variables?

More broadly, this work aims to investigate the mechanisms behind any observed response to test the hypothesis that primary productivity is the first-order driver of fish populations, and to discuss the implications this may have for future climate change.

#### *Research Design*

The research methodology was designed to make use of the most appropriate and easily-obtainable data sources that are available to answer the above questions.

### *Introduction to pelagic ooze records*

Direct evidence of fish populations can be found in deep-sea sediments. Approximately 74% of the ocean floor – or 268 km<sup>2</sup> – is covered with pelagic sediments, very fine-grained deposits composed of debris settling down through the water column. Pelagic “oozes” containing at least 30% organic content make up about two-thirds of this, while the remainder is red clay with less than 30% organic content (Mero, 1965, p. 106). The organic content consists of skeletal remains of microscopic marine organisms, mainly foraminifera tests, diatoms, and calcareous nannofossils like coccoliths (Palmer-Julson and Rack, 1992). Pelagic sediments may also contain fossil fish teeth and other ichthyoliths – significant to this work.

Since 1966, a series of programs have drilled and cataloged cores of deep-sea sediment, starting with the Deep Sea Drilling Project (DSDP) in 1966, the Ocean Drilling Program (ODP) in 1985, the Integrated Ocean Drilling Program (IODP) in 2003, and now the International Ocean Discovery Program (IODP) in 2013 (IODP, 2014).

### *Suitability of core data*

Pelagic sediment cores are uniquely suited to paleoclimate studies due to their high temporal resolution and low spatial resolution:

*High temporal resolution.* Pelagic sediments accumulate slowly but continuously: for highly productive regions, a deposition rate of twenty meters per million years is typical (Palmer-Julson and Rack, 1992), meaning that every centimeter of sediment represents about 500 years of continuous deposition. Because skeletal debris settles rapidly enough (on the order of weeks to years – see, e.g., Popova, 1986) and can

remain virtually undisturbed once deposited, cores of pelagic sediment offer an unprecedented opportunity to collect sequenced historical data on marine chemistry and ecosystems with a resolution of centuries rather than ages.

*Low spatial resolution.* Because individual tests can drift up to 2,500 kilometers from their point of origin (Popova, 1986), pelagic sediment cores represent an average of entire regions of the ocean. This is ideal for studying large-scale climatic variations, as it reduces the likelihood that observed trends are highly localized anomalies.

#### *Site Selection*

This work presents data from three DSDP/ODP/IODP cores containing sediment from the Paleocene-Eocene boundary: ODP 1260B, ODP 1220B, and ODP 1209C. Sites were chosen on the basis of sample availability, geographic location, suitability and resolution of the PETM section in each core, and the existence of prior research such as carbon isotope data. The cores chosen represent one mid-Atlantic site (1260B) and two Pacific sites, one in the Western Pacific (1209C) and one in the Eastern Pacific (1220B). The implications of this geographic spread will be discussed in more detail in chapters 3 and 4.

#### *Procedure*

Ichthyoliths were extracted from ODP/IODP core samples and counted to produce a proxy of regional fish populations. The process of isolating, collecting, and processing the data is explained below.

### *Sample Processing*

Because ichthyoliths make up such a small proportion of the material in a typical pelagic ooze sample, a multi-step process must be used to eliminate as many other constituents as possible. Due to the comparative novelty of this type of processing, it does not presently have a standard operating procedure. The following is a summary of the procedure used for the data in this work, with comments on rationale and lessons learned:

1. *Extraction.* Sediment samples are extracted from the core at specified intervals and bagged separately.
2. *Dehydration.* The samples are dried in low-temperature ovens until their weight stabilizes, indicating that nearly all moisture is gone. This prevents IAR calculations from being biased by variations in water content.
3. *Initial basic data-collection.* Each sample is weighed separately. To calculate ichthyolith accumulation rates (IARs), the density of each sample must be known; basic density data is available from ODP/IODP core records, but if higher resolution density data is needed, additional measurements may be taken. For 1260B, rough volume/density data was obtained through liquid displacement in a graduated cylinder, after manual disaggregation.
4. *Disaggregation.* Unusually hard samples may require manual disaggregation before dissolution to increase surface area. For 1260B, samples were loosely crushed in a mortar before dissolution.
5. *Dissolution.* Samples are soaked in a bath of 5-10% acetic acid until all carbonate constituents are dissolved. Unusually hard or “sticky” samples may require

manual disaggregation during dissolution; using a flat-ended rod with a gentle to moderate pressing and rotating motion was found to be effective. (For 1260B, certain samples could not be disaggregated effectively without excessively damaging the ichthyoliths, and were discarded. A number of approaches were attempted, including ultrasonic disaggregation, stronger acid, and temperature adjustments, but without success.)

6. *Washing.* A standard foram wash is used to remove clay constituents. Samples are transferred to a wet sieve stack (e.g. 150  $\mu\text{m}$  and 38  $\mu\text{m}$  sieves) and washed with running water, gently brushing with the fingers to break up any clumps, until all clay constituents are washed out. Brushing should be as light as possible, to avoid breaking up more delicate ichthyoliths and significantly altering the resulting data – see “1260B Drift Correction,” below.
7. *Drying.* Samples are transferred onto filter paper and dried in low-temperature ovens.
8. *Final basic data-collection.* Once dry, samples are weighed again and transferred to storage vials for future analysis.

Ideally, samples should be processed in random order, or in a systematic but non-sequential order such as a repeated binary division. This makes it possible to spot and correct gradual drifts in processing methodology that might otherwise be lost in the data as a false signal (see “1260B Drift Correction,” below, for a case study).

### *Data Preparation*

Once samples have been processed, they may be separated into manageable size fractions with a dry sieve stack and examined under a microscope. In the case of excessively large samples, a splitter may be used.

The primary data presented in chapter 3 are ichthyolith accumulation rates (IARs) calculated by counting the total number of ichthyoliths larger than 90  $\mu\text{m}$  (for 1260B and 1220B) or 60  $\mu\text{m}$  (for 1209C) and converting to ichthyoliths/ $\text{cm}^2\text{-ka}$  (ichthyoliths per cubic centimeter per thousand years). These data will be discussed in detail in chapters 3 and 4.

### *Staining*

Dissolution and washing eliminate carbonates and clays, but not silica. If there are significant siliceous constituents, such as radiolarians, the difficulty of finding and analyzing ichthyoliths in the sample is increased.

While producing the 1209C and 1220B datasets, Doug Tomczik, Richard Norris, and Elizabeth Sibert developed an optional staining procedure to improve the visual contrast of ichthyoliths against background silica. Ichthyoliths are stained with Alizarin Red S ( $\text{C}_{14}\text{H}_7\text{NaO}_7\text{S}$ ), a calcium stain that selectively colors calcium phosphate pink. This procedure is similar to existing methods for staining fish bones (Green, 1952) or tissue sections (IHC World, 2011).

After dissolution, the acid is partially drained and a solution of Alizarin Red S and distilled water is added to the remaining liquid. The exact ratio of dilute acetic acid, stain, and water is somewhat arbitrary, but guides for tissue staining suggest maintaining a 2% concentration of Alizarin Red S for a staining time of several minutes. Industry



guides recommend maintaining a pH of 4.1-4.3 (e.g., ICH World, 2011), but in practice this does not appear to be critical in this application.

To improve stain clarity, the sample may optionally be soaked in a weak base such as dilute bleach or hydrogen peroxide for a few minutes. Teeth typically stain most deeply near the roots, where the enamel is less dense.

### *1260B Drift Correction*

Analysis of the raw 1260B data revealed a slight downward drift in ichthyolith counts over time, independent of position in the core – e.g., the last 33% of samples processed had total ichthyolith counts significantly ( $p \leq 0.05$ ) lower than the first 33%, even though processing order was selected randomly. This suggests that subjective parts of the processing methodology changed slightly over the course of the project. Experimental testing suggested that the most likely culprit was variations in the pressure of the fingers manipulating the sample while washing it – the more roughly the sediment is handled, the more likely delicate ichthyoliths are to break.

Correction parameters were selected to produce the most uniform mean and median values across the sequence of processing (excluding the anomalously high values during the height of the CIE). The final 1260B data uses a three-part “stepped” correction, chosen as an approximate “best guess” model based on the appearance of the drift trend and laboratory notes, and which provides a more statistically and visually smooth result than a simple linear correction (see figures 1 and 2).

This correction does not change the conclusions given in chapter 4, but does produce a smoother record over short distances – although the uncertainty of the corrected points is unknown, so it would be unwise to give too much weight to apparent

small-scale oscillations. The fact that this correction was even needed emphasizes the importance of consistency and a light touch when washing samples.

#### *Age model*

Age models were derived from two sources: the orbitally-tuned age model developed for ODP 1209 by Westerhold and others (2008), and the independently calibrated  $^3\text{He}$ -tuned age model developed for ODP 1266 by Murphy and others (2010). Models were applied to each site using scaled correlations of each site's  $\delta^{13}\text{C}$  record, processed in AnalySeries 2.0.

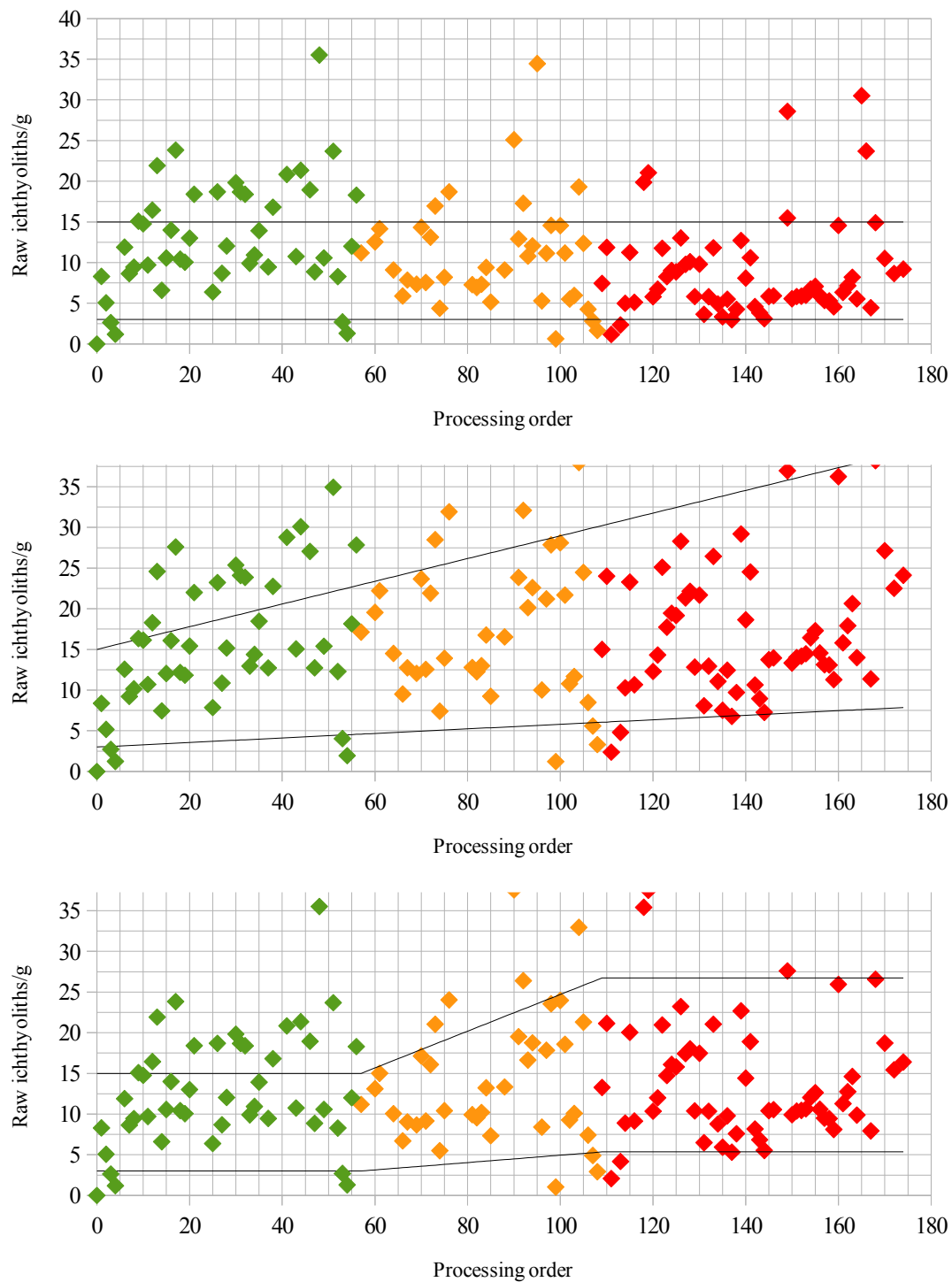


Figure 1: Three correction types for 1260B: uncorrected (top), linear (middle), and stepped (bottom). Lines illustrate the magnitude of correction for each point. First 33% processed are in green, second in yellow, third in red.

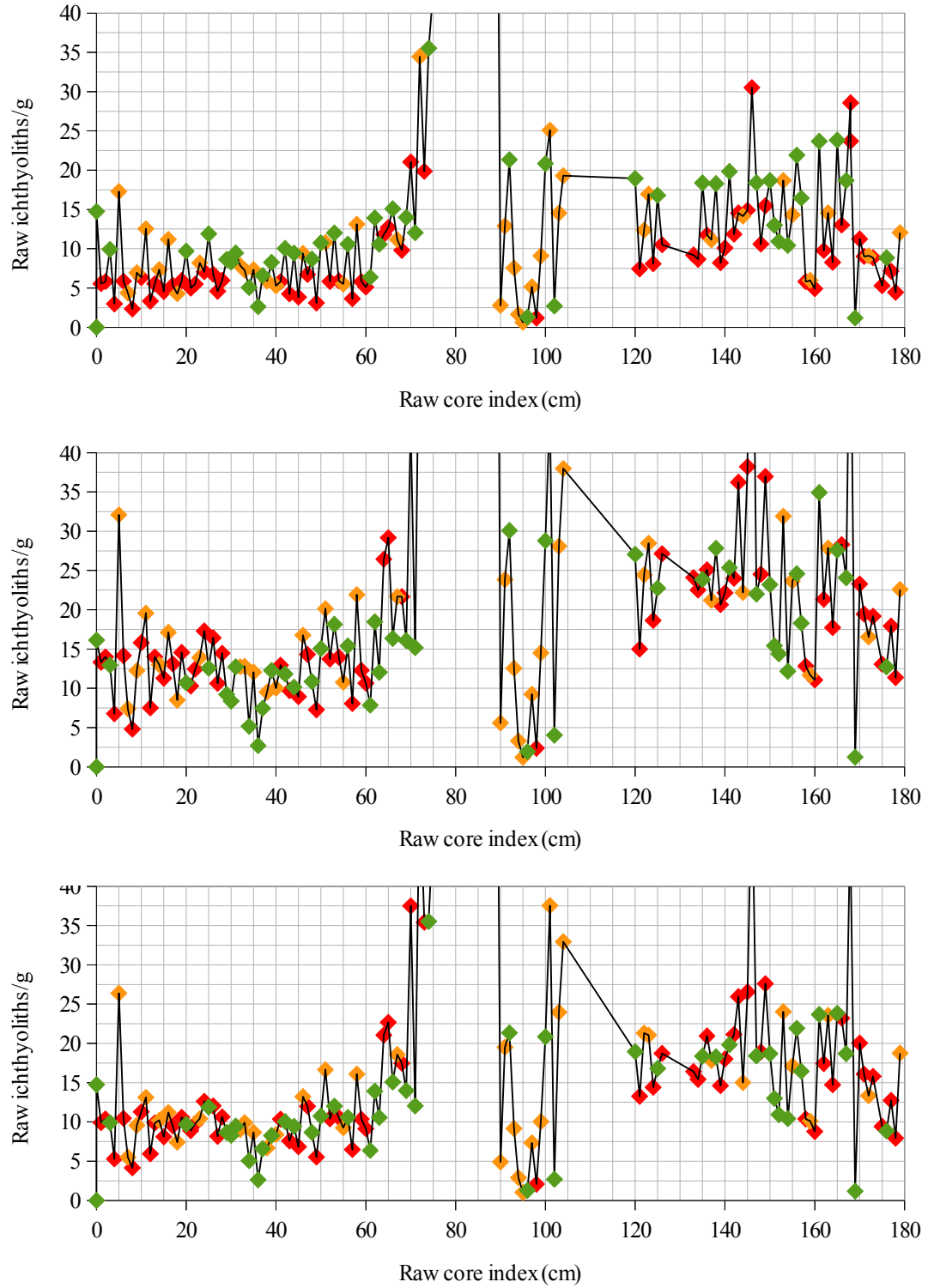


Figure 2: Effects of three correction types for 1260B: uncorrected (top), linear (middle), and stepped (bottom). First 33% processed are in green, second in yellow, third in red.

## CHAPTER THREE

### Results

#### *ODP 1260B*

##### *Sample Background*

ODP Site 1260 is a West Atlantic site, located 2,549 mbsl (meters below sea level) on the northwest-facing slope of Demerara Rise, a prominent submarine plateau off the northern coast of South America (Erbacher and others, 2004). Demerara Rise contains a record of marine sediment from the Early Cretaceous to the present, including a relatively complete Paleogene sequence (Erbacher and others, 2002).

Data were collected from 278.85 to 280.64 meters below sea floor (mbsf) at one-centimeter intervals, with some omissions: the interval from 279.99 to 280.04 mbsf was unavailable; the intervals from 279.90 to 279.98 mbsf and 280.12 to 280.17 mbsf could not be sufficiently disaggregated; and the samples for 279.15, 279.19, 279.21, 279.87, 279.88, 280.07, 280.54, and 280.59 mbsf were omitted from analysis due to contamination, damage, and/or various processing issues. In total, 84% of the core was included in the final analysis. The average sample was 6.5 g of dried sediment.

##### *Summary of Results*

The 1260B dataset has the highest resolution of the three datasets considered, and shows the largest IAR variance. Using the orbitally tuned “Westerhold” age model, late Paleocene IARs have a mean of 42.8 ichthyoliths/cm<sup>2</sup>·ka and a standard deviation of 13.9. Around the onset of the CIE, IAR drops off, reaching a minimum value of 2.3.

(The timing of this event relative to the onset of the CIE is unclear due to the resolution of the carbon isotope data.) IAR subsequently rebounds to a peak value of 994.0, 5,000-15,000 years after the apparent onset of the CIE, then declines over the next 20,000-30,000 years to a more stable Eocene mean of 15.2 with a standard deviation of 6.6.

Due to the magnitude of IAR variance, two sets of figures are provided. Figures 3 and 4 show detail views of the 1260B record in both the Westerhold age model (figure 3) and the Murphy age model (figure 4). Figure 5 shows the complete 1260B record, with both age models side-by-side.

### *ODP 1209C*

#### *Sample Background*

ODP Site 1209 is a West Pacific site, located 2,387 mbsl near the center of Shatsky Rise, a submarine plateau off the southeast coast of Japan. Shatsky Rise contains marine sediment from the Late Cretaceous to the present day, including a Paleocene to Oligocene section that appears largely complete (Bralower and others, 2002).

IARs were obtained from Doug Tomczik. Data were collected from 195.8 to 198.9 mbsf at intervals of 10 cm, with a sample size of approximately 30 cc, representing 2-3 cm of core (Tomczik, 2014).

#### *Summary of Results*

Site 1209 shows a spike similar to 1260B, but much smaller in magnitude. Late Paleocene IARs have a mean of 8.5 ichthyoliths/cm<sup>2</sup>·ka and a standard deviation of 2.5. The peak IAR data point is approximately 8,000 years after the apparent onset of the CIE,

with a value of 53.5; the next data point is approximately 40,000 years later, by which time IARs have declined to a new Eocene mean of 5.4 with a standard deviation of 1.9.

### *ODP 1220B*

#### *Sample Background*

ODP Site 1220 is a Central Pacific site, located 5,218 mbsl in abyssal hill topography approximately 1,600 km southeast of Hawaii. The seafloor basalt is overlaid by approximately 200 m of continuous pelagic sediments, spanning the late Paleocene to early Miocene (Lyle and others, 2002).

IARs were obtained from Richard Norris. Data were collected at irregular intervals of 5-10 cm, with a sample size of approximately 10 cc, representing 2 cm of core per sample.

#### *Summary of Results*

1220B contains few Paleocene data points compared to either 1260B or 1209C. The bulk of the data points show a stable Eocene IAR of 8.6 ichthyoliths/cm<sup>2</sup>·ka, with a standard deviation of 3.7. The available Paleocene and mid-CIE IARs are much higher, with a mean of 54.2 and a standard deviation of 48.2, but lack a clear trend.

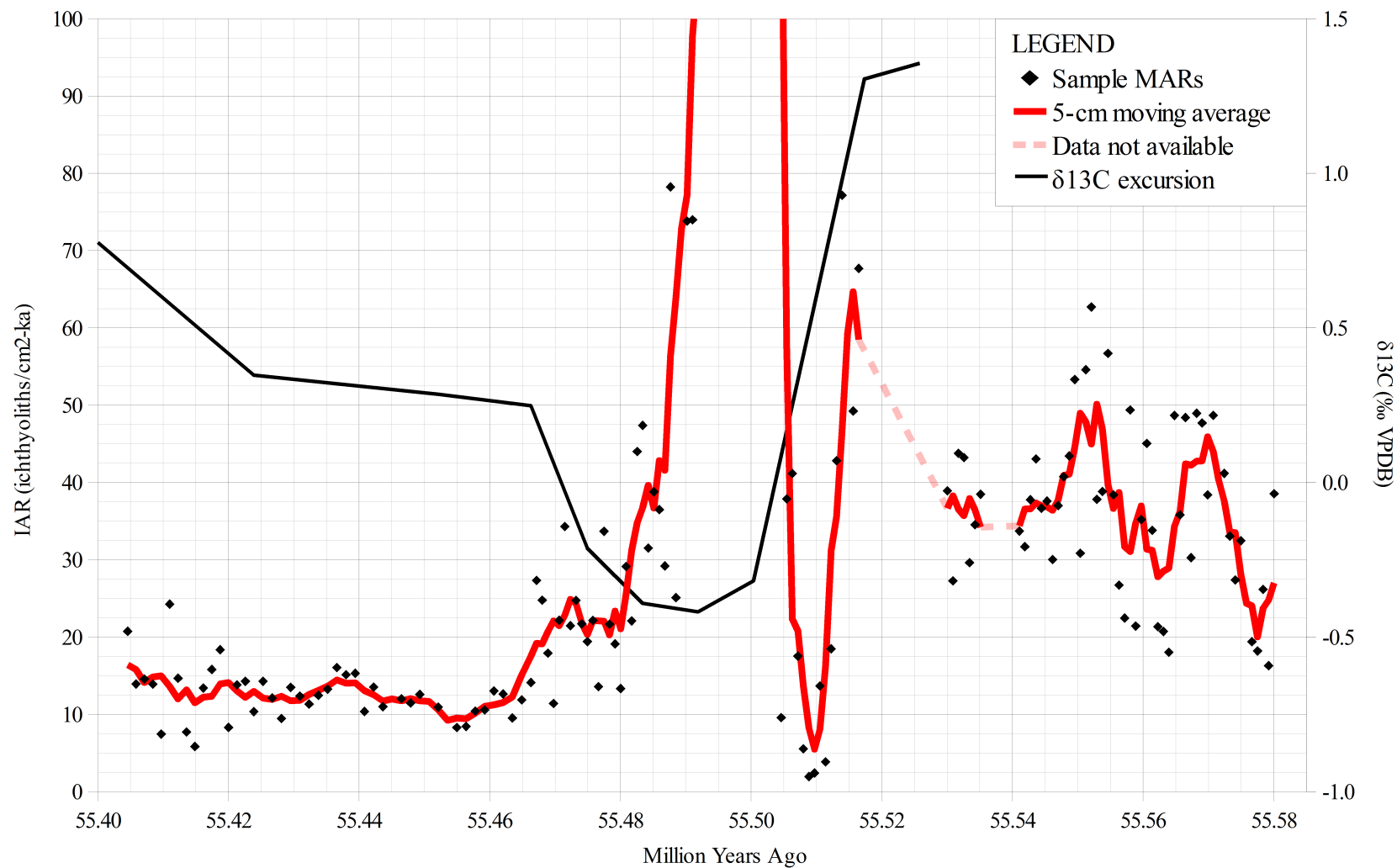


Figure 3: 1260B net IAR (Westerhold timescale) – detail



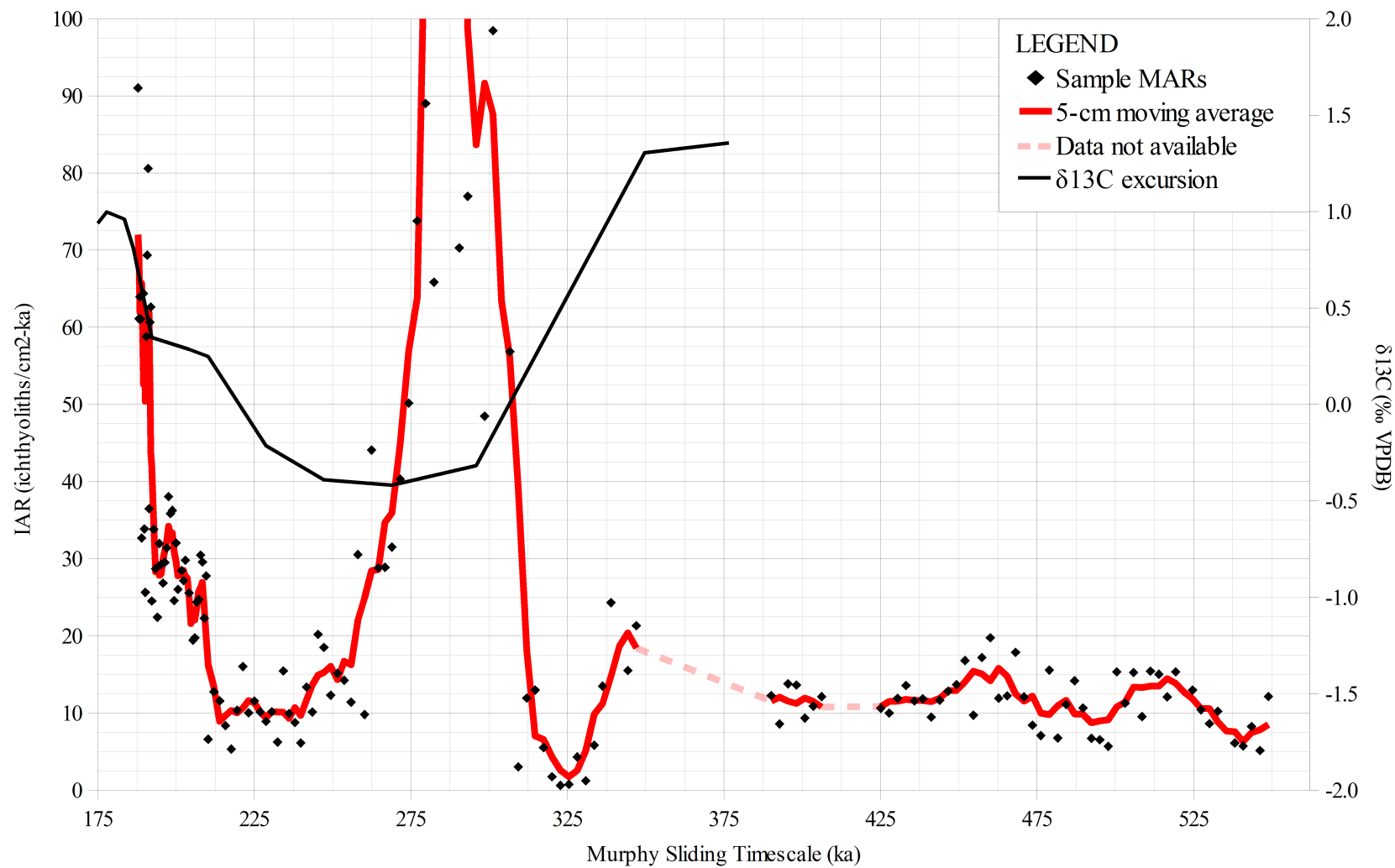


Figure 4: 1260B net IAR (Murphy timescale) – detail

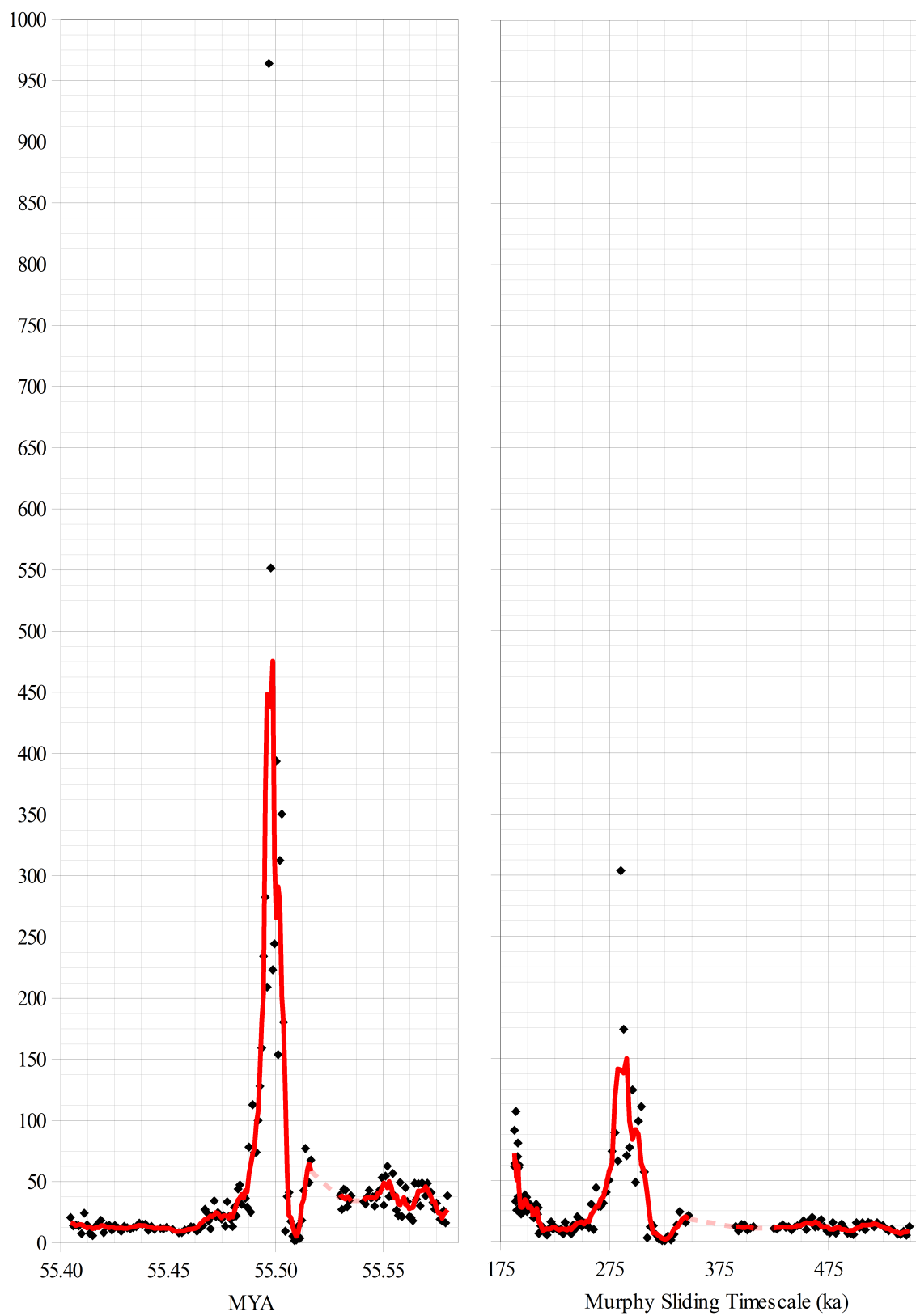


Figure 5: 1260B net IAR – full; left is Westerhold, right is Murphy

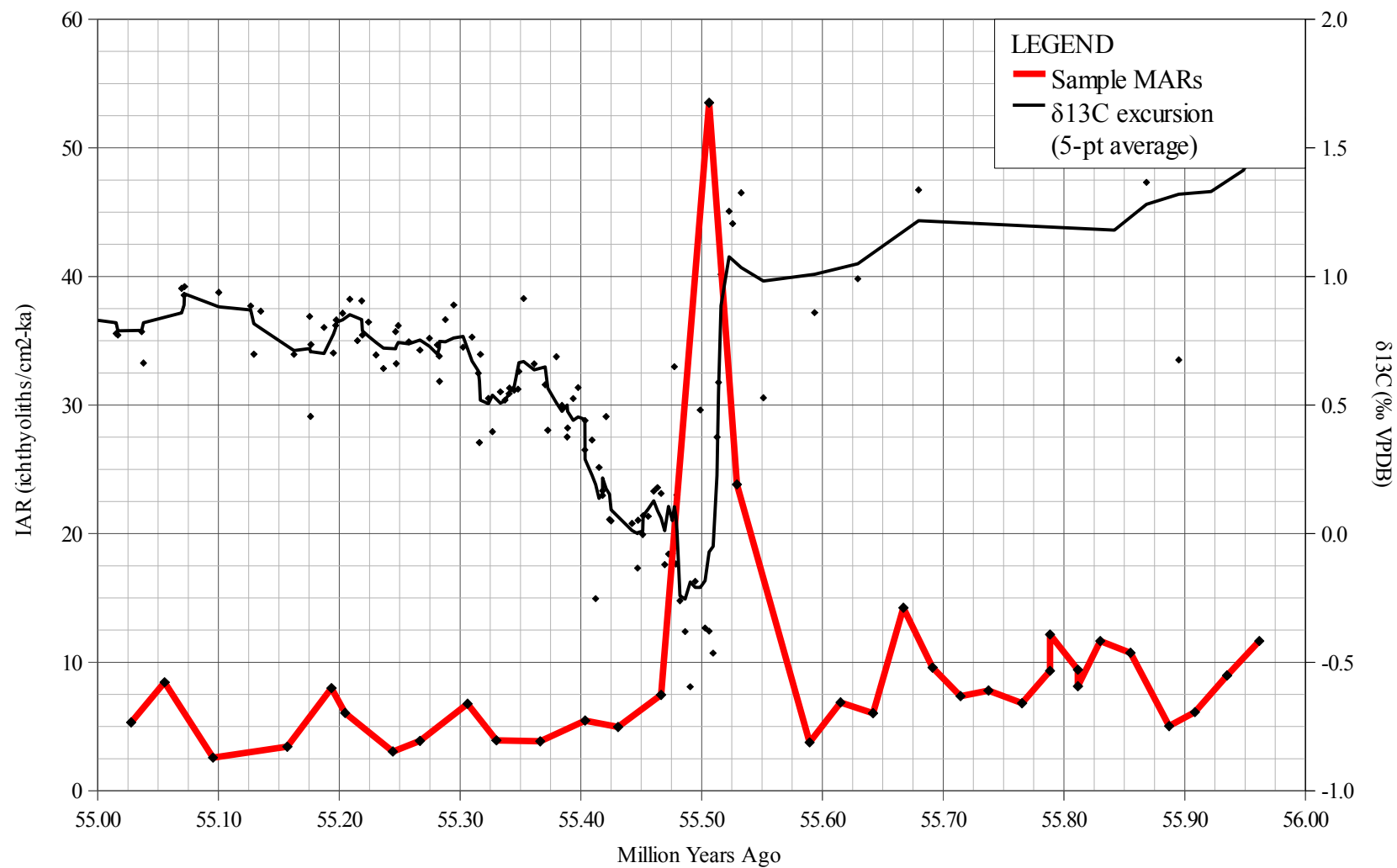


Figure 6: 1209C net IAR

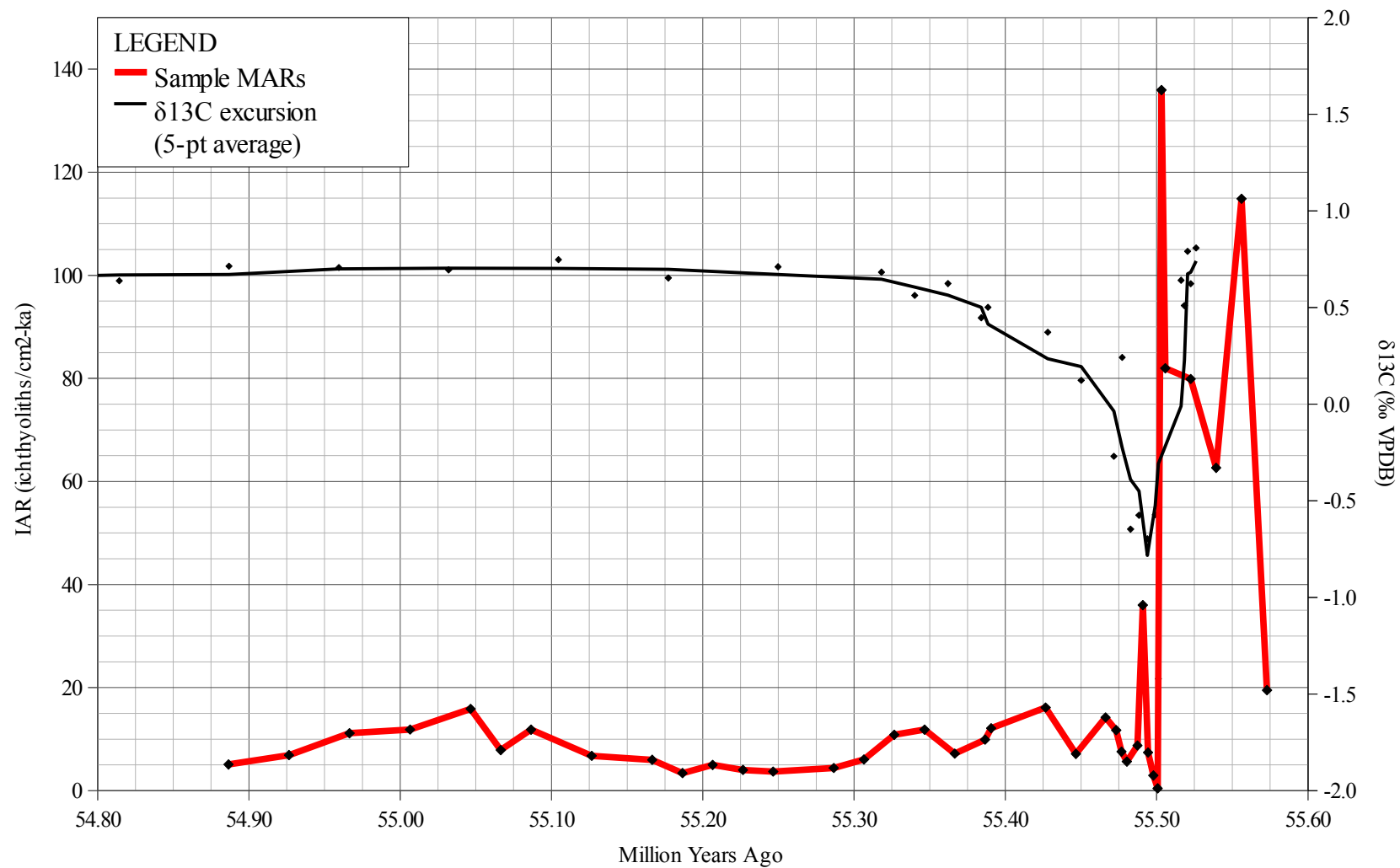


Figure 7: 1220B net IAR

## CHAPTER FOUR

### Interpretation and Discussion

#### *Trends and Concordance*

All three datasets show a statistically significant increase in IAR associated with the CIE, suggesting that warming of the oceans was associated with significantly higher fish productivity in the tens of thousands of years following the onset of the CIE. An estimate of peak productivity falling 10,000 to 15,000 years after the onset of the CIE is consistent with all three datasets.

The data from ODP 1260B suggest that the increase was preceded by a period of below-average fish productivity, at least in the Atlantic, but the 1209C and 1220B records do not have a high enough resolution to determine if productivity declined in the Pacific as well.

#### *ODP 1260B*

The most statistically significant trend is the drop-off and subsequent spike following the CIE, which is apparent under both age models. Smaller-scale IAR trends are ambiguous, however. Using the Westerhold age model, the equilibrium IAR values following the PETM appear to drop by approximately 65% compared to their late-Paleocene values. This effect disappears when using the  $^3\text{He}$  tuned “Murphy” age model. (The Westerhold age model is strongly preferred for analysis – see chapter 2 – but both are provided for purposes of comparison.)

### *ODP 1209C*

While comparison is limited by resolution, the results from 1209C appear consistent with the results from 1260B. Both 1260B and 1209C show a stable Paleocene IAR, spike, and stable Eocene IAR, with similar timing. 1209C shows no evidence of the pre-spike drop-off seen in 1260B, but this may be an artifact of the lower resolution, as the temporal gap between the pre-CIE and peak data points is large enough to completely hide a drop-off.

### *ODP 1220B*

The results from 1220B are broadly consistent with 1260B and 1209C, but differ in certain aspects. The peak IAR value of 136.0 falls within the expected age range – approximately 15,000 years after the apparent onset of the CIE – but the evidence for a gradual drawdown is shaky: the peak value is immediately followed by three data points representing 8,000-10,000 years of low IARs (mean of 3.6). As with 1209C, there is no evidence of the dropoff seen in 1260B, but there is a sufficiently large temporal gap in the data (~17,000 years) to hide it.

### *Age Model Considerations*

The interpretive usefulness of the data presented in Chapter 3 is closely linked to the validity of the age models used to construct it. Potential errors and biases fall mainly into two categories: timing relative to the PETM, and deposition rate.

### *Timeline relative to the PETM*

The timing of population shifts relative to the onset of the PETM has obvious implications for ecological interpretation. Several factors minimize the potential for

timeline error. First, for the models based on stratigraphic indicators (e.g. Westerhold), the onset of the PETM is fixed at the base of the dissolution layer – the accepted stratigraphic marker for the Paleocene-Eocene boundary. Using 1260B as an example, this constrains the possible offset error to within several thousand years (assuming a range of possible deposition rates between 500-3,000 yr/cm). Second, because the given carbon isotope data were obtained from the same cores and use the same age models, the approximate timing of population shifts relative to other events of the PETM is easy to verify.

#### *Deposition rates*

Calculated IARs are highly dependent on the deposition rates derived from the age models. As discussed above, a too-high deposition rate would result in too-low IARs, and vice versa. In theory, sufficient error in the age models could completely reshape the appearance of the population trends.

Error tolerance is hard to determine quantitatively, but a qualitative evaluation suggests that deposition rate error is insufficient to account for the observed trends. The most prominent trend is the “spike” shortly after the onset of the PETM, which appears in all three datasets. In order for this spike to be wholly an artifact of deposition rate, where the actual peak values during the “spike” are no greater than peak values before the spike, calculated deposition rates during the spike would have to be 2.8 times too high for 1209C, 0.18 times too high for 1220B, and 12.3 times too high for 1260B. There is no evidence for such a change, however, and such deposition rates would stretch the timescale and  $\delta^{13}\text{C}$  data beyond the accepted boundaries of the PETM (see, e.g., Röhl and

others, 2007). This suggests that the observed “spikes” cannot be explained by deposition rate alone (with the possible exception of the 1220B record).

### *Taphonomic and Diagenetic Considerations*

Taphonomic and diagenetic factors can introduce bias and false signals into the data. This section discusses several such factors, and the influence they may have.

#### *Bioturbation*

Bioturbation of marine oozes can mix the top tens of centimeters of sediment together (Palmer-Julson and Rack, 1992), complicating interpretation by averaging the record over longer periods of time. The 1209C and 1260B units show evidence of bioturbation (Bralower and others, 2002; Erbacher and others, 2004), but several lines of evidence suggest that none of the records are have been bioturbated/time-averaged over intervals greater than 1-3 cm:

5. All three cores show distinct depositional boundaries at or near the PETM interval, wherein sediment composition changes over an interval of 2 cm or less (figure 8). 1220B in particular shows distinct laminations approximately 1 mm thick (figure 9). Laminations are a strong indicator that bioturbation was minimal (Palmer-Julson and Rack, 1992). However, the sharpness of the dissolution boundary in particular may be a result of penetration depth rather than a lack of bioturbation.
6. The data presented in chapter 3 appear to have a high temporal resolution. For example, immediately following the P/E boundary in the 1260B record, net



IAR drops nearly 95% within 3 cm. If the 1260B record were time-averaged over intervals greater than 1-3 cm, this drop-off would occur more slowly.

7. The depositional environments of 1209C, 1220B, and 1260B typically have low bioturbation. Bioturbation is strongly affected by deposition rate: the slower the rate of deposition, the less benthic food is buried beneath the surface, leading to shallower burrowing. Because deposition rate generally decreases further offshore, deep-ocean oozes can have a very thin zone of bioturbation (Wetzel, 1984).

#### *Pellet decomposition*

Biogenic material settles to the seafloor in three main ways: directly; as constituents of fecal pellets; and as constituents of marine snow (Palmer-Julson and Rack, 1992). Fecal pelletization is the main route for the settling of smaller particles, such as coccoliths. Tests are ingested by pelagic predators (such as copepods and shrimp) and excreted in fecal pellets, which sink much more quickly than normal tests – as fast as 360 m/day (Popova 1986), a journey of days versus years. Marine snow is similar to pelletization, but forms naturally as inorganic clumps (or flocs) of tests, clay, pellets, and other material (Palmer-Julson & Rack 1992). Larger tests such as radiolarians often settle directly, as fast as 70 m/day (Popova 1986).



Figure 8: Core sections, left to right: ODP 1209C-11H section 2, 3, and 4; ODP 1220B-20X section 1 and 2; and ODP 1260B-17R section 6 and 7.



Figure 9: Detail of ODP 1220B-20X-02, showing laminations.

Experiments have shown that acidification can significantly slow pelletization as dissolution of carbonate ballast reduces settling time and increases residence time in the water column, where the pellets are continuously degraded (de Jesus Mendes and Thomsen, 2012). Elevated temperatures appear to accelerate both aggregate formation and degradation through increased bacteria growth and feeding (Piontek and others, 2009). However, surface waters may not have acidified significantly during the PETM, and carbonate production does not appear to have slowed significantly (Gibbs and others, 2010).

Despite these uncertainties, pellet degradation seems unlikely to be a primary factor in the observed IAR data, for two reasons. First, ichthyoliths are large enough to settle directly without difficulty, reducing the impact of pellet degradation. Second, reduced transport would cause measured IARs to be lower than actual fish productivity;

while this may partially explain the dropoff seen in 1260B, it does not explain the apparent IAR “spikes”, which still fall within the dissolution interval.

### *Dissolution*

The PETM interval is characterized by carbonate dissolution from rapid shoaling of the CCD (Zachos and others, 2005). This dissolution has the potential to disrupt ichthyolith data in two ways: first, by changing the apparent deposition rate (and thus IARs), and second, by directly contributing to ichthyolith breakdown. (Issues of deposition rate will be covered below, under “Age Model Considerations.”)

Visual observations on 1260B did not suggest that ichthyoliths were significantly more degraded during the dissolution interval. Chemically, the difference is small: Penman and others (2014) calculate a pH drop of 0.3 from pre-PETM levels between 7.5 and 8.2, a difference that does not (by itself) cause a sharp increase in the solubility of calcium phosphate (Goss and others, 2007) – although more complex factors affecting diagenetic disarticulation or sample processing are harder to rule out. In particular, Palmer-Julson and Rack (1992) suggest that dissolution may increase the ease of fragmentation in diatoms.

If acidification during the PETM did significantly degrade or fragment ichthyoliths, measured IARs would be lower than actual fish productivity. As above, however, this does not explain the apparent IAR “spikes.”

### *Primary Productivity as a Driver*

As discussed in detail in chapter 1, there is an increasing consensus that primary productivity rose in the recovery stages of the PETM, likely as a result of elevated nutrient flux from increased terrigenous runoff. While the increase in primary productivity roughly coincides with the increase in fish productivity, it does not appear sufficient to explain it.

The effect of primary productivity on fish populations can be estimated with a simple trophic model. The total biomass that can be sustained at a given trophic level by a given level of primary productivity, at a given transfer efficiency, is

$$BM_i = BM_{NPP} \times TE^{TL_i}$$

where  $BM_{NPP}$  is primary productivity biomass,  $BM_i$  is the biomass of level  $i$ ,  $TE$  is transfer efficiency, and  $TL_i$  is the trophic level of level  $i$ .

The mean trophic level of commercially-fished species in the early 1950's was slightly more than 3.3 (Pauly and others, 1998). Transfer efficiency between trophic levels is often assigned a universal constant of 10%, but this figure represents a hypothetical median value with little empirical support (Slobodkin, 2001). Libralato and others (2008) found a global mean transfer efficiency of 12% for fisheries, ranging from a high of 14% on temperate shelves to a low of 5% in upwelling zones.

Because  $TE^{TL_i}$  is effectively a constant for global fish population, this shows that the percent change in sustainable fish biomass is equivalent to the percent change in primary productivity.

Ma and others (2014) reports primary productivity proxy data from twelve DSDP/ODP sites, based on barite accumulation rates (figures 10). To convert barium

data from Ma and others' sliding timescale to an absolute timescale, a value of 55.514 mya was selected as the start of the CIE, based on the overlap of possible values from each core. The expected range of uncertainty in Ma and others' selection of a CIE start point is too small to substantially alter the results below.

Quantitatively, regression plots do not show a strong or consistent correlation between IAR and interpolated barium accumulation rate (BAR) (figure 11).

Qualitatively, the magnitude and timing of variation in barium flux occasionally appears consistent with the magnitude and timing of variation in the ichthyolith data, but the data are incomplete at best and show additional trends not observed in the ichthyolith data.

These analyses suggest that, while productivity may be a factor, it is not the only driving force behind the observed population fluctuations.

#### *ODP 1209A*

Data from 1209A begins nearly 12,000 years after the onset of the CIE, so it cannot be compared to the main spike in 1209C. The barite record includes three “spikes” of its own, however: a data point 500% above background values around 50,000 years, a data point 550% above background around 100,000 years, and a data point 290% above background at 145,000 years. The 1209C fish record has no corresponding increases.

#### *ODP 1220B*

IAR peaks at 1,580% of its pre-CIE value approximately 15,000 years after the onset of the CIE. The barite productivity proxy peaks at 2,180% of its average pre-CIE value approximately 5,000-15,000 years after the onset of the CIE. Neither record

appears to show a gradual drawdown; however, the barite proxy records a second spike of 1,600% approximately 85,000 years after the onset of the CIE, which does not appear in the ichthyolith record.

#### *ODP 1260B*

The nearest barite record from Ma and others (2014) is ODP 1051B, off the southeastern coast of North America. 1051B does show a spike, but the magnitude is much smaller (110% versus 2,300%) and the onset is much later (25,000-30,000 years versus 5,000-15,000 years).

#### *Discussion*

Interpretation is hampered by inconsistency between sites, the lack of control data from outside the PETM, and age model differences between this work and Ma and others (2014). As such, this should be seen as preliminary exploratory work. However, taken together with prior biotic and chemical work (e.g. Gibbs and others, 2006), these data do suggest that primary productivity may have peaked after fish productivity.

This may suggest that fish productivity peaked in a “sweet spot” of warm, oligotrophic conditions, after the onset of warming but before increased eutrophication from phytoplankton activity. Further work could investigate this hypothesis.

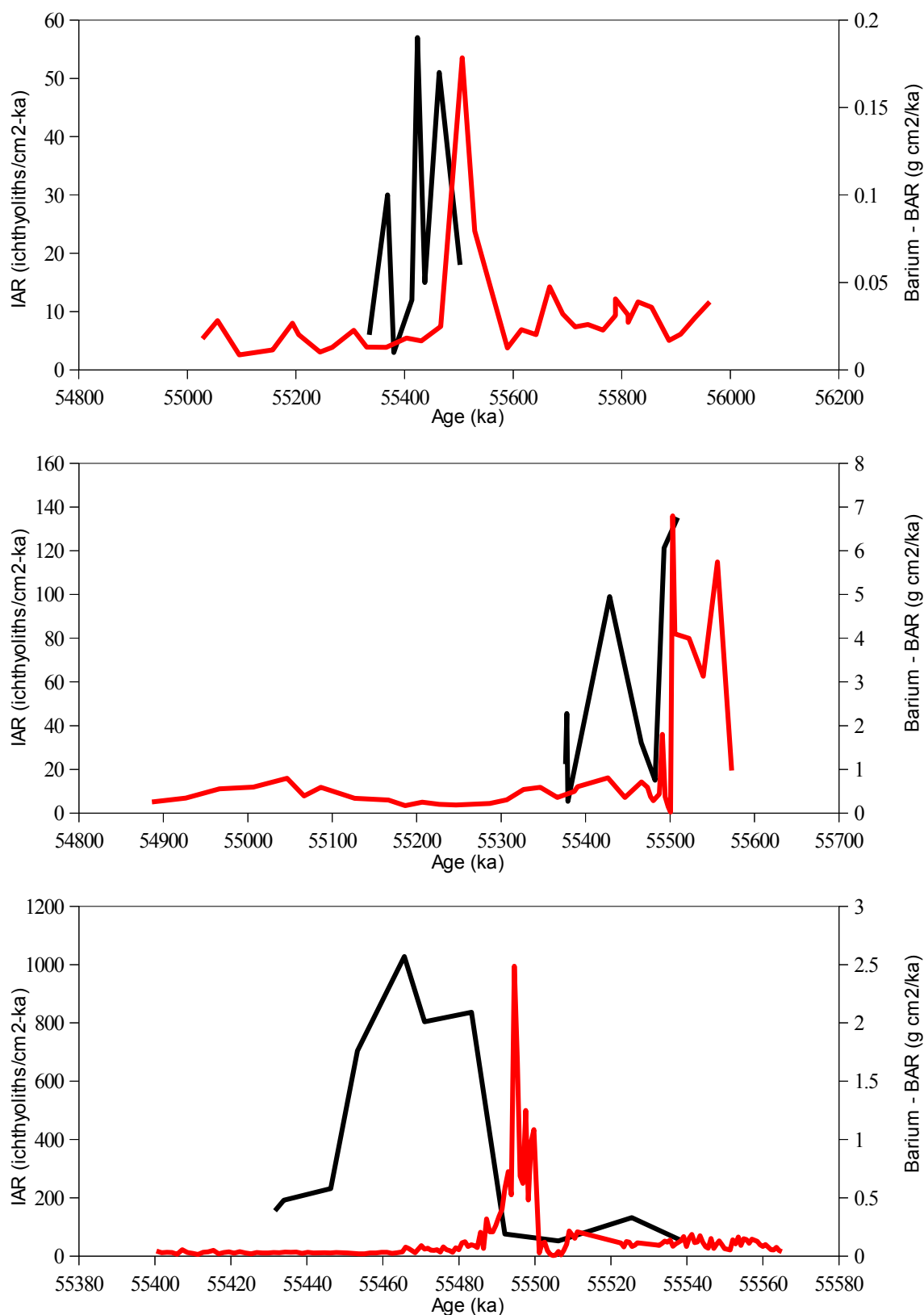


Figure 10: Ichthyoliths (red) vs. Ba (black) – from top: 1209C, 1220B, and 1260B/1051B



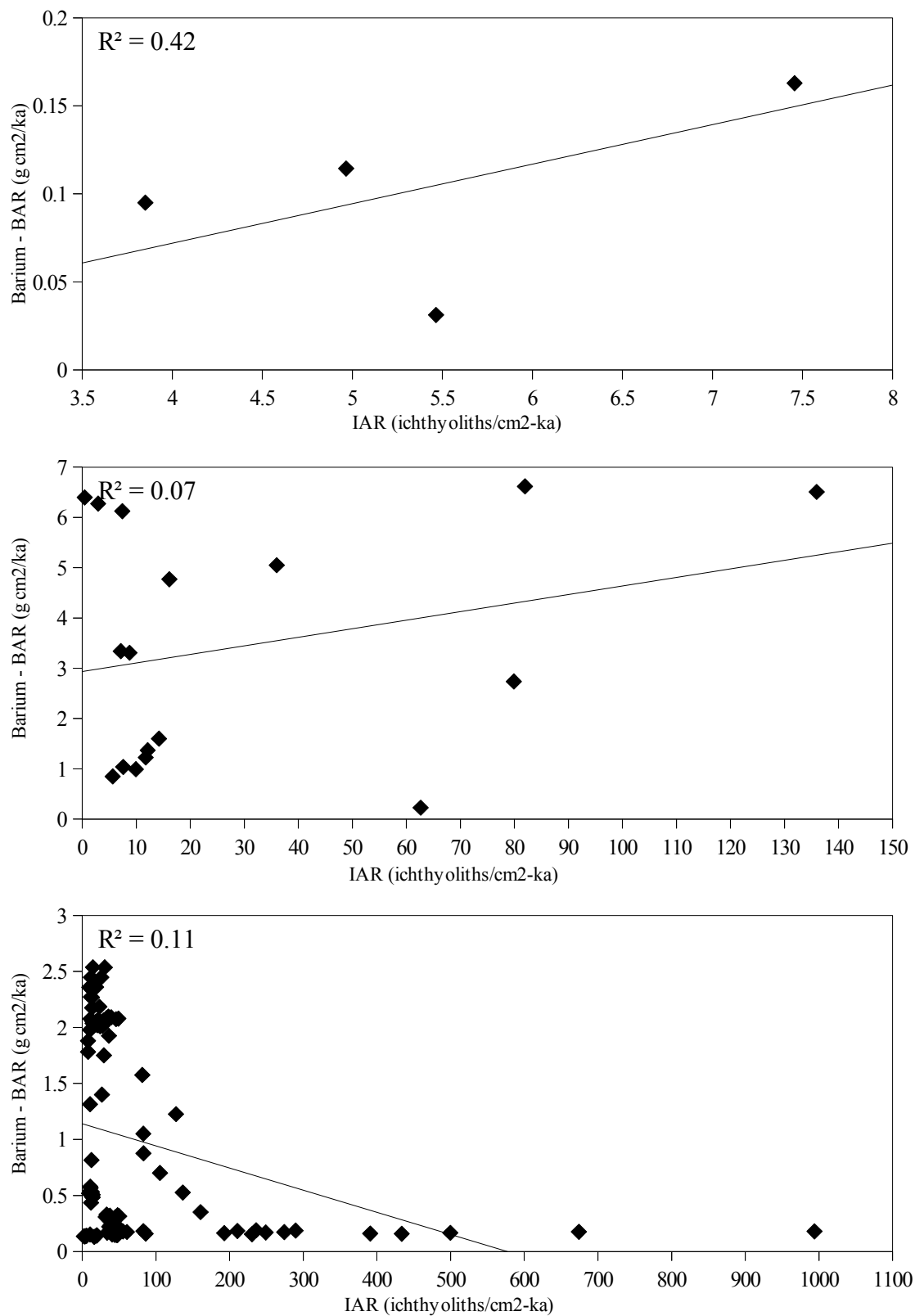


Figure 11: Ichthyoliths versus barium – from top: 1209C, 1220B, and 1260B/1051B

## CHAPTER FIVE

### Conclusion

The results of this research are both hopeful and concerning. It appears that, historically, fish have been able to adapt to – and even thrive in – a warmer climate, developing highly productive ecosystems over a period of tens of thousands of years. At the same time, the highest-resolution data available suggest that this long-term productivity was preceded by a short-term crash, at least in the Atlantic. While a mere hiccup from a geologic perspective, the prospect of hundreds of years of severely depleted fish populations could be devastating from a human perspective.

Several factors complicate how directly these results can be used to predict future ecosystems. First, the PETM is not a perfect analogue to future climate change. Because future climate change is expected to occur much more rapidly than during the PETM, ecological disruption may be much greater (Haywood and others, 2011). This may affect the mechanism of population shifts as well as the magnitude, making the eventual response entirely unpredictable. If, however, the observed population trends are understood as inevitable equilibrium responses to the changed climate, the rate of warming becomes less important.

Second, the mechanism is not fully understood. The most obvious driver, primary productivity, does not appear sufficient to explain the observed trends; but more broadly, research concerning the impact of climate change on fish has generally focused on short-term effects, i.e. within the next few decades or centuries (IPCC, 2014, ch. 6 and 30). Little is known about how global fish populations will behave over millennia.

Third, fish populations may be significantly affected by factors that may not translate directly to the modern era. For example, differences in the shape and size of the Atlantic basin between the Eocene and the Holocene could affect ocean circulation patterns, which in turn could affect population dynamics. However, the presence of comparable trends in both the Atlantic and Pacific suggest that population shifts in the PETM were not driven solely by localized factors.

Further research is needed to investigate the causes of PETM fish trends. For now, the fundamental message of the PETM is clear: the impacts of climate change are significant and wide-ranging, and that the oceans of the future may look very different from the oceans of the present.

## BIBLIOGRAPHY

- Alegret, L., S. Ortiz, I. Arenillas, and E. Molina, 2010, What happens when the ocean is overheated? The foraminiferal response across the Paleocene–Eocene Thermal Maximum at the Alamedilla section (Spain): *Geological Society of America Bulletin*, v. 122, no. 9-10, p. 1616–1624, doi:10.1130/B30055.1.
- Allison, E. H. et al., 2009, Vulnerability of national economies to the impacts of climate change on fisheries: *Fish and Fisheries*, v. 10, no. 2, p. 173–196, doi:10.1111/j.1467-2979.2008.00310.x.
- Bains, S., R. D. Norris, R. M. Corfield, and K. L. Faul, 2000, Termination of global warmth at the Palaeocene/Eocene boundary through productivity feedback: *Nature*, v. 407, no. 6801, p. 171–174, doi:10.1038/35025035.
- Bains, S., R. D. Norris, R. M. Corfield, G. J. Bowen, P. D. Gingerich, and P. L. Koch, 2003, Marine-terrestrial linkages at the Paleocene-Eocene boundary: Special Paper - *Geological Society of America*, v. 369, p. 1–9.
- Berggren, W. A., and K. Ouda, 2003, Upper Paleocene-lower Eocene planktonic foraminiferal biostratigraphy of the Dababiya section, Upper Nile Valley (Egypt): *Micropaleontology*, v. 49, no. Suppl 1, p. 61–92, doi:10.2113/49.Suppl\_1.61.
- Bornemann, A., P. Schulte, J. Sprong, E. Steurbaut, M. Youssef, and R. P. Speijer, 2009, Latest Danian carbon isotope anomaly and associated environmental change in the southern Tethys (Nile Basin, Egypt): *Journal of the Geological Society*, v. 166, no. 6, p. 1135–1142, doi:10.1144/0016-76492008-104.
- Bralower, T. J., 2002, Evidence of surface water oligotrophy during the Paleocene-Eocene thermal maximum: Nannofossil assemblage data from Ocean Drilling Program Site 690, Maud Rise, Weddell Sea: *Paleoceanography*, v. 17, no. 2, p. 13–1, doi:10.1029/2001PA000662.
- Bralower, T. J., I. Premoli Silva, and M. Malone, 2002, Site 1209, in *Proceedings of the Ocean Drilling Program: Initial Reports*.
- Burgess, G., 1901, A Permutative System, in *The Burgess Nonsense Book: Being a Complete Collection of the Humorous Masterpieces of Gelett Burgess*. Frederick A. Stokes Company.

- Cecil, C. B., and F. T. Dulong, 2003, Precipitation Models for Sediment Supply in Warm Climates, in *Climate Controls on Stratigraphy*: Society for Sedimentary Geology, p. 21–27.
- Charles, A. J., D. J. Condon, I. C. Harding, H. Pälike, J. E. A. Marshall, Y. Cui, L. Kump, and I. W. Croudace, 2011, Constraints on the numerical age of the Paleocene-Eocene boundary: Geochemistry, Geophysics, Geosystems, v. 12, no. 6, p. n/a–n/a, doi:10.1029/2010GC003426.
- De Jesus Mendes, P. A., and L. Thomsen, 2012, Effects of Ocean Acidification on the Ballast of Surface Aggregates Sinking through the Twilight Zone: PLoS ONE, v. 7, no. 12, p. e50865, doi:10.1371/journal.pone.0050865.
- Dickens, G. R., T. Fewless, E. Thomas, and T. J. Bralower, 2003, Excess barite accumulation during the Paleocene-Eocene Thermal Maximum: Massive input of dissolved barium from seafloor gas hydrate reservoirs, in *Causes and Consequences of Globally Warm Climates in the Early Paleogene*: Geological Society of America.
- Erbacher, J., D. Mosher, J. Bauldauf, and M. Malone, 2002, Demerara Rise: Equatorial Cretaceous and Paleogene Paleooceanographic Transect, Western Atlantic, in *Leg 207 Scientific Prospectus*: Ocean Drilling Program.
- Erbacher, J., D. Mosher, and M. Malone, 2004, Site 1260, in *Proceedings of the Ocean Drilling Program: Initial Reports*.
- FAO, 2012, *The State of World Fisheries and Aquaculture 2012*: FAO Fisheries and Aquaculture Department, Food and Agriculture Organization of the United Nations.
- Gibbs, S. J., H. M. Stoll, P. R. Bown, and T. J. Bralower, 2010, Ocean acidification and surface water carbonate production across the Paleocene–Eocene thermal maximum: *Earth and Planetary Science Letters*, v. 295, no. 3–4, p. 583–592, doi:10.1016/j.epsl.2010.04.044.
- Gibbs, S. J., T. J. Bralower, P. R. Bown, J. C. Zachos, and L. M. Bybell, 2006, Shelf and open-ocean calcareous phytoplankton assemblages across the Paleocene-Eocene Thermal Maximum: Implications for global productivity gradients: *Geology*, v. 34, no. 4, p. 233–236, doi:10.1130/G22381.1.
- Gingerich, P. D., 2006, Environment and evolution through the Paleocene–Eocene thermal maximum: *Trends in Ecology & Evolution*, v. 21, no. 5, p. 246–253, doi:10.1016/j.tree.2006.03.006.

- Giusberti, L., D. Rio, C. Agnini, J. Backman, E. Fornaciari, F. Tateo, and M. Oddone, 2007, Mode and tempo of the Paleocene-Eocene thermal maximum in an expanded section from the Venetian pre-Alps: *Geological Society of America Bulletin*, v. 119, no. 3-4, p. 391–412, doi:10.1130/B25994.1.
- Goss, S. L., K. A. Lemons, J. E. Kerstetter, and R. H. Bogner, 2007, Determination of calcium salt solubility with changes in pH and PCO<sub>2</sub>, simulating varying gastrointestinal environments: *Journal of Pharmacy and Pharmacology*, v. 59, no. 11, p. 1485–1492, doi:10.1211/jpp.59.11.0004.
- Green, M. C., 1952, A Rapid Method for Clearing and Staining Specimens for the Demonstration of Bone: *The Ohio Journal of Science*, v. 52, no. 1.
- Hönisch, B. et al., 2012, The Geological Record of Ocean Acidification: *Science*, v. 335, no. 6072, p. 1058–1063, doi:10.1126/science.1208277.
- Haywood, A. M., A. Ridgwell, D. J. Lunt, D. J. Hill, M. J. Pound, H. J. Dowsett, A. M. Dolan, J. E. Francis, and M. Williams, 2011, Are there pre-Quaternary geological analogues for a future greenhouse warming?: *Philosophical Transactions of the Royal Society A: Mathematical, Physical and Engineering Sciences*, v. 369, no. 1938, p. 933–956, doi:10.1098/rsta.2010.0317.
- ICH World, 2011, Alizarin Red S Staining Protocol for Calcium: ICH World Life Science Products & Services:  
<[http://www.ichworld.com/\\_protocols/special\\_stains/alizarin\\_red\\_s.htm](http://www.ichworld.com/_protocols/special_stains/alizarin_red_s.htm)>  
(accessed November 25, 2014).
- IODP, 2014, History: <<http://www.iodp.org/history>> (accessed November 25, 2014).
- IPCC, 2014, Fifth Assessment Report: United Nations Intergovernmental Panel on Climate Change.
- Kaiho, K., K. Takeda, M. R. Petrizzo, and J. C. Zachos, 2006, Anomalous shifts in tropical Pacific planktonic and benthic foraminiferal test size during the Paleocene–Eocene thermal maximum: *Palaeogeography, Palaeoclimatology, Palaeoecology*, v. 237, no. 2–4, p. 456–464, doi:10.1016/j.palaeo.2005.12.017.
- Kelly, D. C., T. J. Bralower, and J. C. Zachos, 1998, Evolutionary consequences of the latest Paleocene thermal maximum for tropical planktonic foraminifera: *Palaeogeography, Palaeoclimatology, Palaeoecology*, v. 141, no. 1–2, p. 139–161, doi:10.1016/S0031-0182(98)00017-0.
- Kelly, D. C., J. C. Zachos, T. J. Bralower, and S. A. Schellenberg, 2005, Enhanced terrestrial weathering/runoff and surface ocean carbonate production during the recovery stages of the Paleocene-Eocene thermal maximum: *Paleoceanography*, v. 20, no. 4, p. PA4023, doi:10.1029/2005PA001163.

- Khozyem, H., T. Adatte, J. E. Spangenberg, A. A. Tantawy, and G. Keller, 2013, Palaeoenvironmental and climatic changes during the Palaeocene–Eocene Thermal Maximum (PETM) at the Wadi Nukhul Section, Sinai, Egypt: *Journal of the Geological Society*, v. 170, no. 2, p. 341–352, doi:10.1144/jgs2012-046.
- Kump, L. R., S. L. Brantley, and M. A. Arthur, 2000, Chemical Weathering, Atmospheric CO<sub>2</sub>, and Climate: *Annual Review of Earth and Planetary Sciences*, v. 28, no. 1, p. 611–667, doi:10.1146/annurev.earth.28.1.611.
- Libralato, S., M. Coll, S. Tudela, I. Palomera, and F. Pranovi, 2008, Novel index for quantification of ecosystem effects of fishing as removal of secondary production: *Marine Ecology Progress Series*, v. 355, p. 107–129, doi:10.3354/meps07224.
- Lyle, M., P. A. Wilson, T. R. Janecek, and et al., 2002, Site 1220, in *Proceedings of the Ocean Drilling Program: Initial Reports*.
- Ma, Z., E. Gray, E. Thomas, B. Murphy, J. Zachos, and A. Paytan, 2014, Carbon sequestration during the Palaeocene-Eocene Thermal Maximum by an efficient biological pump: *Nature Geoscience*, v. 7, no. 5, p. 382–388, doi:10.1038/ngeo2139.
- McInerney, F. A., and S. L. Wing, 2011, The Paleocene-Eocene Thermal Maximum: A Perturbation of Carbon Cycle, Climate, and Biosphere with Implications for the Future: *Annual Review of Earth and Planetary Sciences*, v. 39, no. 1, p. 489–516, doi:10.1146/annurev-earth-040610-133431.
- Mero, J. L., 1965, *The Mineral Resources of the Sea*: Elsevier, 327 p.
- Murphy, B. H., K. A. Farley, and J. C. Zachos, 2010, An extraterrestrial <sup>3</sup>He-based timescale for the Paleocene–Eocene thermal maximum (PETM) from Walvis Ridge, IODP Site 1266: *Geochimica et Cosmochimica Acta*, v. 74, no. 17, p. 5098–5108, doi:10.1016/j.gca.2010.03.039.
- Norris, R. D., S. K. Turner, P. M. Hull, and A. Ridgwell, 2013, Marine Ecosystem Responses to Cenozoic Global Change: *Science*, v. 341, no. 6145, p. 492–498, doi:10.1126/science.1240543.
- Nunes, F., and R. D. Norris, 2006, Abrupt reversal in ocean overturning during the Palaeocene/Eocene warm period: *Nature*, v. 439, no. 7072, p. 60–63, doi:10.1038/nature04386.
- Ouda, K., and W. A. Berggren, 2003, Biostratigraphic correlation of the Upper Paleocene-Lower Eocene succession in the Upper Nile Valley: A synthesis: *Micropaleontology*, v. 49, no. Suppl 1, p. 179–212, doi:10.2113/49.Suppl\_1.179.

- Ouda, K., W. A. Berggren, and K. Saad, 2003, The Gebel Owaina and Kilabiya sections in the Idfu-Esna area, Upper Nile Valley (Egypt): *Micropaleontology*, v. 49, no. Suppl 1, p. 147–166, doi:10.2113/49.Suppl\_1.147.
- Palmer-Julson, A., and F. R. Rack, 1992, The relationship between sediment fabric and planktonic microfossil taphonomy; how do plankton skeletons become pelagic ooze? *PALAIOS*, v. 7, no. 2, p. 167–177, doi:10.2307/3514927.
- Pauly, D., V. Christensen, J. Dalsgaard, R. Froese, and F. Torres, 1998, Fishing Down Marine Food Webs: *Science*, v. 279, no. 5352, p. 860–863, doi:10.1126/science.279.5352.860.
- Penman, D. E., B. Hönisch, R. E. Zeebe, E. Thomas, and J. C. Zachos, 2014, Rapid and sustained surface ocean acidification during the Paleocene-Eocene Thermal Maximum: *Paleoceanography*, p. 2014PA002621, doi:10.1002/2014PA002621.
- Piontek, J., N. Hndel, G. Langer, J. Wohlers, U. Riebesell, and A. Engel, 2009, Effects of rising temperature on the formation and microbial degradation of marine diatom aggregates: *Aquatic Microbial Ecology*, v. 54, no. 3, p. 305–318, doi:10.3354/ame01273.
- Popova, I. M., 1986, Transportation of radiolarian shells by currents (calculations based on the example of the Kuroshio): *Marine Micropaleontology*, v. 11, no. 1–3, p. 197–201, doi:10.1016/0377-8398(86)90014-9.
- Röhl, U., T. Westerhold, T. J. Bralower, and J. C. Zachos, 2007, On the duration of the Paleocene-Eocene thermal maximum (PETM): *Geochemistry, Geophysics, Geosystems*, v. 8, no. 12, p. n/a–n/a, doi:10.1029/2007GC001784.
- Ravizza, G., R. N. Norris, J. Blusztajn, and M.-P. Aubry, 2001, An osmium isotope excursion associated with the Late Paleocene thermal maximum: Evidence of intensified chemical weathering: *Paleoceanography*, v. 16, no. 2, p. 155–163, doi:10.1029/2000PA000541.
- Schenau, S. J., and G. J. D. Lange, 2000, A Novel Chemical Method to Quantify Fish Debris in Marine Sediments: *Limnology and Oceanography*, v. 45, no. 4, p. 963–971.
- Slobodkin, L. B., 2001, The good, the bad and the reified: *Evolutionary Ecology Research*, v. 3, no. 1, p. 1–13.
- Soliman, M. F., 2003, Chemostratigraphy of the Paleocene/Eocene (P/E) boundary sediments at Gabal el-Qreiya, Nile Valley, Egypt: *Micropaleontology*, v. 49, no. Suppl 1, p. 123–138, doi:10.2113/49.Suppl\_1.123.



- Stoll, H. M., N. Shimizu, D. Archer, and P. Ziveri, 2007, Coccolithophore productivity response to greenhouse event of the Paleocene–Eocene Thermal Maximum: Earth and Planetary Science Letters, v. 258, no. 1–2, p. 192–206, doi:10.1016/j.epsl.2007.03.037.
- Tantawy, A. A. A. M., 2006, Calcareous nannofossils of the Paleocene-Eocene transition at Qena Region, Central Nile Valley, Egypt: Micropaleontology, v. 52, no. 3, p. 193–222, doi:10.2113/gsmicropal.52.3.193.
- Thomas, E., 2007, Cenozoic mass extinctions in the deep sea: What perturbs the largest habitat on Earth?, in S. Monechi, R. Coccioni, and M. R. Rampino, eds., Large Ecosystem Perturbations: Causes and Consequences: Geological Society of America.
- Tomczik, D. W., 2014, Fish Production and Diversity across the Paleocene-Eocene Thermal Maximum: Evidence for Enhanced Export Production and Community Resilience: UNIVERSITY OF CALIFORNIA, SAN DIEGO.
- Torfstein, A., G. Winckler, and A. Tripathi, 2010, Productivity feedback did not terminate the Paleocene-Eocene Thermal Maximum (PETM): Climate of the Past, v. 6, p. 265–272.
- Westerhold, T., U. Röhl, H. K. McCarren, and J. C. Zachos, 2009, Latest on the absolute age of the Paleocene–Eocene Thermal Maximum (PETM): New insights from exact stratigraphic position of key ash layers +19 and –17: Earth and Planetary Science Letters, v. 287, no. 3–4, p. 412–419, doi:10.1016/j.epsl.2009.08.027.
- Westerhold, T., U. Röhl, I. Raffi, E. Fornaciari, S. Monechi, V. Reale, J. Bowles, and H. F. Evans, 2008, Astronomical calibration of the Paleocene time: Palaeogeography, Palaeoclimatology, Palaeoecology, v. 257, no. 4, p. 377–403, doi:10.1016/j.palaeo.2007.09.016.
- Wetzel, A., 1984, Bioturbation in deep-sea fine-grained sediments: influence of sediment texture, turbidite frequency and rates of environmental change: Geological Society, London, Special Publications, v. 15, no. 1, p. 595–608, doi:10.1144/GSL.SP.1984.015.01.37.
- Zachos, J. C. et al., 2005, Rapid Acidification of the Ocean During the Paleocene-Eocene Thermal Maximum: Science, v. 308, no. 5728, p. 1611–1615, doi:10.1126/science.1109004.
- Zamagni, J., M. Mutti, and A. Košir, 2012, The evolution of mid Paleocene-early Eocene coral communities: How to survive during rapid global warming: Palaeogeography, Palaeoclimatology, Palaeoecology, v. 317–318, p. 48–65, doi:10.1016/j.palaeo.2011.12.010.